



# Identifying Li<sup>+</sup> ion transport properties of aluminum doped lithium titanium phosphate solid electrolyte at wide temperature range



Shaofei Wang, Liubin Ben, Hong Li\*, Liquan Chen

Institute of Physics, Chinese Academy of Sciences, Beijing 100190, China

## ARTICLE INFO

### Article history:

Received 3 June 2014

Received in revised form 29 September 2014

Accepted 7 October 2014

Available online 24 October 2014

### Keywords:

Lithium titanium phosphate

Al-doping

Low temperature

Bulk conductivity

Grain boundary conductivity

Impedance analysis

## ABSTRACT

A series of  $\text{Li}_{1+x}\text{Al}_x\text{Ti}_{2-x}(\text{PO}_4)_3$  samples ( $x = 0\text{--}0.4$ ) were prepared by solid state reaction and were characterized. Lattice parameters  $a$  and  $c$  decrease continuously with increase of Al content. The relative density of the Al-doped samples is about 97%, which is much higher than 75% of the undoped  $\text{LiTi}_2(\text{PO}_4)_3$  sample. Detailed ac impedance measurements from  $-150$  °C to  $60$  °C reveal clearly that three electrical response regions with different relaxation time constants coexist in the undoped  $\text{LiTi}_2(\text{PO}_4)_3$  sample but only two in all Al-doped samples. The bulk ionic conductivities for the Al-doped samples show no significant variation from  $x = 0.1$  to  $x = 0.4$ . Their ionic conductivities are slightly higher than those of the undoped sample. However, this increase is not caused by increasing bulk ionic conductivity through introducing more lithium ions via doping, but it is mainly attributed to a densification effect.

© 2014 Elsevier B.V. All rights reserved.

## 1. Introduction

Lithium ion battery technology is now being widely pursued for vehicle and grid applications [1]. All solid-state batteries with solid electrolyte are expected to solve the safety problem of lithium ion batteries. Solid electrolyte needs to meet several requirements, including high ionic conductivity, high lithium ion transference number, wide electrochemical window, low electronic conductivity, low interfacial resistance, high stability during fabrication, operation and storage, moderate mechanical properties, low cost, nontoxic and easy handling [2].  $\text{LiM}_2(\text{PO}_4)_3$  ( $M = \text{Ge, Ti, Sn, Zr, and Hf}$ ) with Na superionic conductor (NASICON) structure has been extensively studied as a promising solid electrolyte [3]. Among these materials,  $\text{LiTi}_2(\text{PO}_4)_3$  (LTP) and its derivatives are particularly attractive due to the high ionic conductivity, high stability, relatively low cost and abundant natural sources [4]. Aono et al. demonstrated that the conductivity of  $\text{LiTi}_2(\text{PO}_4)_3$  at room temperature ( $2 \times 10^{-6} \text{ S cm}^{-1}$ ) could be greatly enhanced by substituting  $\text{Ti}^{4+}$  with trivalent cations such as  $\text{Al}^{3+}$ ,  $\text{Ga}^{3+}$ ,  $\text{Cr}^{3+}$ ,  $\text{In}^{3+}$ ,  $\text{Sc}^{3+}$ ,  $\text{Fe}^{3+}$ , and  $\text{Y}^{3+}$ . A maximum conductivity of  $7 \times 10^{-4} \text{ S cm}^{-1}$  was obtained in  $\text{Li}_{1.3}\text{M}_{0.3}\text{Ti}_{1.7}(\text{PO}_4)_3$  ( $M = \text{Al or Sc}$ ) at room temperature (298 K) [5]. Although much effort has been done to raise the ionic conductivity of  $\text{LiTi}_2(\text{PO}_4)_3$  by Al-doping (LATP), the conductivity enhancement mechanism is still in dispute [4].

Previous studies have shown that the grain boundary conductivity significantly contributes to the total conductivity [5]. It is clear that the Al-doping can increase the grain boundary conductivity, while its influence on the bulk conductivity was not confirmed [5,6]. It has been suggested that Al-doping can enhance the bulk ionic conductivity from  $1 \times 10^{-4} \text{ S cm}^{-1}$  in  $\text{LiTi}_2(\text{PO}_4)_3$  to  $3 \times 10^{-3} \text{ S cm}^{-1}$  in  $\text{Li}_{1.3}\text{Al}_{0.3}\text{Ti}_{1.7}(\text{PO}_4)_3$  [5]. It seems that the bulk conductivity is dependent on the grain boundary conductivity, as further studied by Aono et al. on  $\text{LiTi}_2(\text{PO}_4)_3$  mixed with lithium salt ( $\text{Li}_3\text{PO}_4$ ,  $\text{Li}_3\text{BO}_3$ ) [7].

As the characteristic relaxation frequency of bulk is very high, the identification of bulk conductivity is actually limited by a usual impedance spectroscopy instrument at room temperature [6]. In order to probe the bulk conductivity with maximum information, K. Arbi et al. performed the impedance testing on  $\text{Li}_{1+x}\text{Al}_x\text{Ti}_{2-x}(\text{PO}_4)_3$  at 150 K–300 K ( $x = 0.05, 0.1, 0.2, 0.5$  and  $0.7$ ). When  $x$  was above 0.2, Al could not be doped in the NASICON structure. For  $x = 0.05$ ,  $x = 0.1$  and  $x = 0.2$ , the measured bulk conductivities were  $2.3 \times 10^{-3} \text{ S cm}^{-1}$ ,  $2.2 \times 10^{-3} \text{ S cm}^{-1}$  and  $5.1 \times 10^{-3} \text{ S cm}^{-1}$ , respectively. The related activation energy decreased from 0.33 eV to 0.30 and 0.28 eV respectively [8,9]. These results seem to support that the bulk conductivity of LTP can be increased after Al-doping.

The  $^7\text{Li}$  NMR study of  $\text{Li}_{1+x}\text{Al}_x\text{Ti}_{2-x}(\text{PO}_4)_3$  shows that the line width of resonance lines changes little when the substitution of Ti by Al increases, which indicates that the ability of lithium motion changes little by Al-doping [10,11]. Nuspl et al. simulated the diffusion of lithium ions in stoichiometric  $\text{LiTi}_2(\text{PO}_4)_3$  and Al-doped  $\text{LiTi}_2(\text{PO}_4)_3$  by the molecular dynamics method using specialized force fields. The simulation

\* Corresponding author. Tel.: +86 10 82648067; fax: +86 10 82649046.  
E-mail address: [hli@iphy.ac.cn](mailto:hli@iphy.ac.cn) (H. Li).

obtained a 0.3 eV bulk activation energy for LTP. The authors drew a conclusion from their simulation that the substitution of Ti for Al within the framework will only slightly influence the activation energy of lithium migration if the changing lithium content is neglected [12].

In view of charge compensation, the substitution of  $x$   $[\text{Ti}^{4+}]$  by  $x$   $[\text{Al}^{3+}]$  will increase  $x$   $[\text{Li}^+]$  naturally, as confirmed by the experimental studies. The conductivity is determined by both concentration and mobility of the mobile charge carrier. Above inconsistency on the Al-doping effect on the bulk conductivity of LTP raises the interests naturally.

The impedance spectroscopy technology at wide temperature range could be particularly powerful in distinguishing the electrical regions from different contributions, such as bulk, grain boundary, surface layer, and sample–electrode contact of materials [13]. In this paper, a series of Al-doped  $\text{LiTi}_2(\text{PO}_4)_3$  have been synthesized and then investigated using impedance spectroscopy between 123 K and 333 K to clarify whether Al-doping can improve the bulk conductivity of  $\text{LiTi}_2(\text{PO}_4)_3$ .

## 2. Experimental

### 2.1. Synthesis of $\text{Li}_{1+x}\text{Al}_x\text{Ti}_{2-x}(\text{PO}_4)_3$

The undoped sample  $\text{LiTi}_2(\text{PO}_4)_3$  (LTP) and the doped sample  $\text{Li}_{1+x}\text{Al}_x\text{Ti}_{2-x}(\text{PO}_4)_3$  (LATP- $x$ ) were prepared by solid state reaction. The stoichiometric mixtures of  $\text{Li}_2\text{CO}_3$ ,  $\text{TiO}_2$ ,  $(\text{NH}_4)_2\text{H}(\text{PO}_4)_3$ , and  $\text{Al}_2\text{O}_3$  were ground for 1 h in an agate mortar. The ground mixtures were heated at 450 °C for 1.5 h followed by 900 °C for 2 h with a heating rate of 3 °C/min in air. The heated mixtures were ball-milled for 8 h. The ball-milled powder was pressed into pellets in a cold die and sintered at 1000 °C for 2 h in the flow of  $\text{O}_2$ .

### 2.2. XRD

The phase assemblage and purity of sintered samples were examined at room temperature using a Bruker D8 Advance diffractometer with  $\text{Cu-K}\alpha$  radiation and a LYNXEYE detector. Data were taken in the range of 10°–80° with 0.02° per step and a count rate of 0.5 s at each step. Lattice parameters were deduced by fitting the XRD pattern with the FullProf program.

### 2.3. XPS

The valence state of Ti in the samples was investigated by X-ray photoelectron spectroscopy (XPS) using an ESCAL 220i-XL electron spectrometer, operating with a monochromated Al-K $\alpha$  X-ray radiation source in a base pressure of  $10^{-7}$  Pa. The spectra were calibrated with respect to the C 1s peak resulting from the adventitious hydrocarbon, which has an energy of 284.6 eV.

### 2.4. SEM

The microstructure of samples was studied by a Hitachi S4800 scanning electron microscope (SEM).

### 2.5. Impedance spectroscopy

Ac impedance measurement was carried out using a NOVO control analyzer. The frequency range was from 1 Hz to 10 MHz and the temperature range was from 123 K to 333 K. The measurement was performed at every 30 K. The temperature was hold for 40 min before each measurement.

## 3. Results and discussions

### 3.1. X-ray diffraction pattern

The XRD patterns of  $\text{Li}_{1+x}\text{Al}_x\text{Ti}_{2-x}(\text{PO}_4)_3$  ( $x = 0$ –0.4) are given in Fig. 1. All samples are pure phase and can be indexed to the R-3C space group in accordance with the previous report [8]. The lattice parameters  $a$  and  $c$  decrease continuously with increasing  $x$  (in Fig. 2), indicating that larger  $\text{Ti}^{4+}$  ( $r_6 = 0.605$  Å) is indeed substituted by smaller  $\text{Al}^{3+}$  ( $r_6 = 0.535$  Å) [14]. The dependence of lattice parameters on  $x$  satisfies Vegard's law very well.

### 3.2. SEM and relative density of ceramics

Fig. 3 shows the cross-section view of the LATP samples. The average grain size of LTP is 1–4  $\mu\text{m}$ . After doping, grains grow to 10–40  $\mu\text{m}$  for all LATP samples. The pores in the LATP samples are much less than those in the LTP samples. Fig. 3(f) shows the relative density of the LATP samples. The relative density was calculated through the apparent density divided by the crystal density. The apparent density was got from the weight divided by the apparent volume. The LTP has a relative density of ~75%. After Al-doping, the relative density of LTP increases to ~97% for  $x = 0.1$ –0.4 in agreement with previous report [5].

### 3.3. XPS of LATP

XPS studies for all samples are shown in Fig. 4. All the samples show similar XPS results. The peak position of Ti  $2p_{3/2}$  peak is centered at 459.7 eV, which represents  $\text{Ti}^{4+} 2p_{3/2}$  [15]. None of our samples show identified signals at the binding energy of 457.6 eV, which is the characteristic peak of  $\text{Ti}^{3+}$  [16,17]. Accordingly, it is clear that there is no sign of  $\text{Ti}^{3+}$  in the sample. It means that the ionic conduction is the conduction mechanism in all the samples.

### 3.4. Ac impedance spectra of LATP

The electrical responses of ceramics can be divided into several electrical regions, such as bulk, grain boundary, surface layer, and sample–electrode interface [13]. Each electrical region has a characteristic relaxation time constant and can be characterized by a resistance ( $R$ ) and a capacitance ( $C$ ), usually placed in parallel. The characteristic relaxation time,  $\tau$ , of each ‘parallel RC element’ is given by the product of  $R$  and  $C$  (Eq. 1) [13].

$$\tau = RC \quad (1)$$

The relaxation frequency ( $f = 1/\tau$ ) is dependent on temperature since both  $R$  and  $C$  are dependent on temperature [13,18–20]. As the

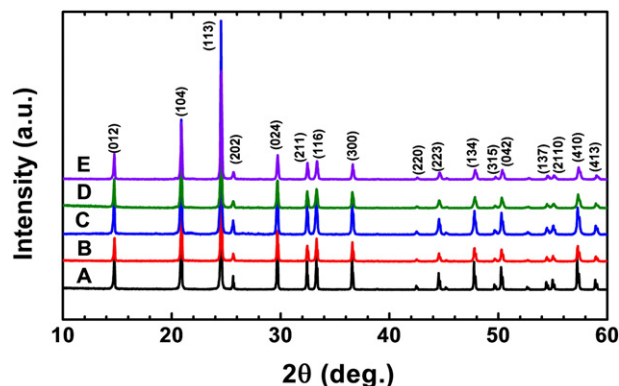


Fig. 1. XRD patterns of different Al-doped samples: (A)  $\text{LiTi}_2(\text{PO}_4)_3$ ; (B)  $\text{Li}_{1.1}\text{Al}_{0.1}\text{Ti}_{1.9}(\text{PO}_4)_3$ ; (C)  $\text{Li}_{1.1}\text{Al}_{0.2}\text{Ti}_{1.8}(\text{PO}_4)_3$ ; (D)  $\text{Li}_{1.3}\text{Al}_{0.3}\text{Ti}_{1.7}(\text{PO}_4)_3$ ; (E)  $\text{Li}_{1.4}\text{Al}_{0.4}\text{Ti}_{1.6}(\text{PO}_4)_3$ .

Download English Version:

<https://daneshyari.com/en/article/1295369>

Download Persian Version:

<https://daneshyari.com/article/1295369>

[Daneshyari.com](https://daneshyari.com)